

One-dimensional diffusion-limited staging transition in graphite intercalation compounds

R. Nishitani, Y. Sasaki, and Y. Nishina

Institute for Materials Research, Tohoku University, Katahira, Sendai 980, Japan

(Received 10 September 1987)

The staging kinetics of the H_2SO_4 graphite intercalation compounds is studied by means of time- and space-resolved Raman scattering measurements. The motion of the phase boundary and the stage distribution is expressed as a function of the degree of supersaturation of the stage-1 phase which is in contact with the reservoir of intercalant (H_2SO_4 liquid). This staging kinetics is described in terms of one-dimensional diffusion in a multiphase system with moving phase boundaries. The present work also explains the time dependence of the domain-pattern formation in the intercalation process.

The kinetic process of the first-order phase transition in a multiphase system is a subject of essential importance in the physics of the pattern formation. The graphite intercalation compound (GIC) presents an example of such systems.

A GIC consists of a periodic arrangement of n graphitic carbon layers and an intercalated layer.¹⁻⁵ This structure is called stage n . Depending on the chemical potential of GIC, it exhibits a phase transition in which the stage index n changes into $n \pm 1$.¹⁻⁸ A great deal of recent interest in the physics of GIC has been focused on the kinetic process of this staging transition. Several experimental⁶⁻¹⁵ and theoretical¹⁶⁻²¹ works have been performed to analyze this process. Kirczenow¹⁹ has carried out a Monte Carlo simulation of staging kinetics in three dimensions. The results reveal clearly the formation process of the stage domain as conceived by Daumas and Herold.²² His results, however, cannot be applied to describe our time-dependent data of the stage-domain distribution¹³ because the Monte Carlo steps are nonlinearly correlated to the real time scale. Furthermore, the scaling law may not hold for the stage-pattern distribution along the lateral plane. We have recently shown that the staging transition proceeds via movement of the narrow phase boundary between well-staged regions of different stage indices.¹³ The domains of different stage numbers are separated macroscopically by the phase boundary, and the boundary moves toward the inner region of the crystal along its c face during the course of the staging transition. GIC's in the process of the staging transition, therefore, form a multiphase system with phase boundaries moving in the sample.

In this paper, we analyze the kinetics of the staging transition in H_2SO_4 GIC's. The result shows that the boundary motion depends on the degree of supersaturation of a well-staged region. For the first time, the time and space dependence of the stage transformation is explained quantitatively in terms of the one-dimensional diffusion of intercalants in a multiphase system.

The time- and space-resolved Raman scattering measurements of H_2SO_4 GIC's during staging transitions are carried out to study *in situ* staging kinetics. The Raman

scattering spectrum due to the graphite intralayer mode ($\sim 1600 \text{ cm}^{-1}$) is monitored to probe the stage structure since the spectrum exhibits stage-dependent Raman shifts.^{23,12,13} The H_2SO_4 GIC is prepared from a highly oriented pyrolytic graphite (HOPG) of its dimensions $\sim 12 \times 4 \times 0.1 \text{ mm}^3$ by an electrochemical method.^{12,13} In the present work, only a sample edge (an area of $\sim 4 \times 0.1 \text{ mm}^2$) is in contact with the H_2SO_4 liquid so that the intercalation reaction takes place only through the interface (a face of the specimen) with the liquid. Raman scattering spectra are measured through the optical multichannel analyzer (OMA) system with a two-dimensional detector of a vidicon with silicon intensified target (SIT). This method enables us to obtain time-resolved spectra at four different positions on the c face in 47 sec in the Raman-shift range from 1350 to 1750 cm^{-1} with the spectral resolution of 0.8 cm^{-1} . Experimental details are described elsewhere.^{13,24}

Figure 1 shows a typical example of time- and space-dependent Raman spectra during intercalation. In each row of Fig. 1, we display a set of Raman spectra at four different positions with a spatial resolution of 0.33 mm . They show the evolution of the graphitic intralayer in the region from 1560 through 1660 cm^{-1} . The characteristic features of time and space dependence of the staging transition, which have been observed previously¹³ as well as in this study, are summarized as follows. (1) Suppose the sample consists entirely of a stage- n domain in contact with the intercalant reservoir. The staging transition from stage n to $n-1$ begins at the interface between the intercalant reservoir and the a face of the GIC sample. (2) The lower stage- $(n-1)$ domain emerges at the interface and proceeds toward the inner region of the crystal. (3) The phase boundaries between domains of different-stage number move toward the inner region as the staging transition progresses.

In order to clarify staging kinetics, we have made above measurements as a function of the degree of supersaturation (DSS) of the stage-1 phase, which is defined as $\Delta\mu/\mu_0 = (\mu - \mu_0)/\mu_0$, where μ_0 is the electrochemical potential at phase boundary between stages 2 and 1 in an equilibrium phase diagram, and μ is the electrochemical

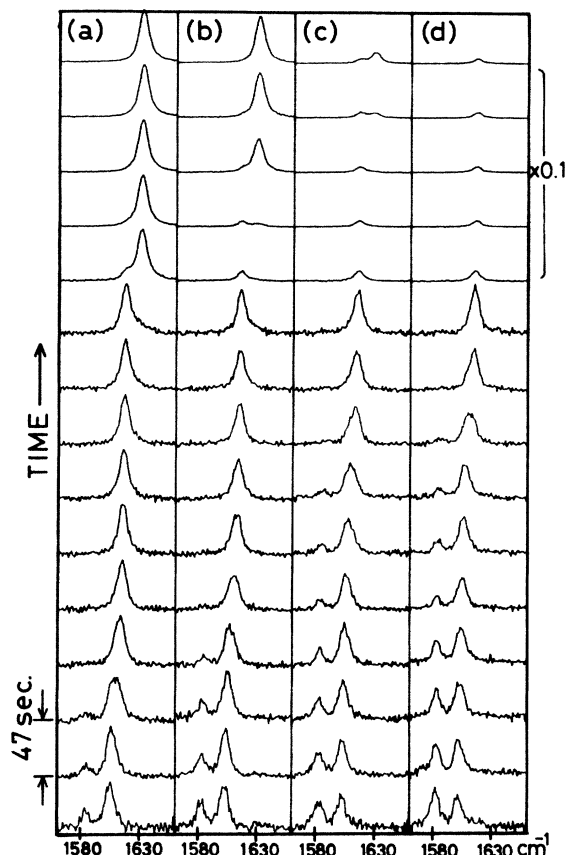


FIG. 1. The time evolution of Raman spectra at four different positions [columns (a)–(d)] with the spatial resolution of 0.33 mm for the graphitic intralayer modes in the region from 1560 through 1660 cm^{-1} during intercalation from graphite through stage 1. All spectra in each of the four panels are measured simultaneously in 47 sec.

potential of the intercalant reservoir (H_2SO_4 liquid). The sample is initially a piece of HOPG. The time-dependent Raman spectra are measured after the electrochemical potential is set at μ with respect to the reference electrode in a stable region of the stage 1.

In Fig. 2(a), we plot a dimensionless parameter of the boundary motion as a function of the degree of supersaturation (DSS). The filled circles show a supersaturation dependence of the boundary motion, $\gamma_1 = \xi_1/2\sqrt{D_1 t}$, between stages 1 and 2. Here ξ_1 is the location of the phase boundary between stages 1 and 2 at time t after the onset of intercalation reaction. The open circles show that of the boundary motion, $\gamma_2 = \xi_2/2\sqrt{D_2 t}$, between the stage-2 domain and the stage-3 domain. Here ξ_2 is the location of the phase boundary at time t . D_i ($i=1,2$) is the diffusion constant of intercalants in a stage- i phase. In Fig. 2(b), we plot the ratio of the depth of the stage-2 region to that of the stage-1 region along the c plane, $(\xi_2 - \xi_1)/\xi_1$, as a function of DSS.

We now show that the results of staging kinetics shown in Figs. 2(a) and 2(b) are well-described by a model of one-dimensional (1D) diffusion in a system consisting of three phases with two moving boundaries. The math-

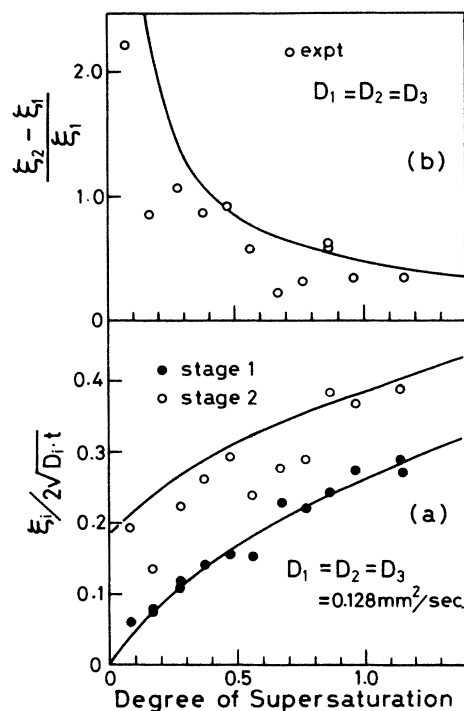


FIG. 2. (a) The coefficients of the motion of the boundaries between stage-1 and stage-2 regions (filled circles), and between stage-2 and higher-stage regions (open circles), as functions of the degree of supersaturation (DSS) for the stage-1 phase. Solid lines are calculated results (see text). (b) The ratio of the depth of the stage-2 region to that of the stage-1 region as a function of DSS. Solid line is the calculated result (see text).

ematics of a diffusion problem in a two-phase system with one moving boundary has been treated by Wagner.²⁵ We have extended the problem to the three-phase system with two moving boundaries. The present model of staging transition is shown in Fig. 3. We assume that the intercalant reservoir is placed at $x < 0$ and is in contact with the a face of the crystal at $x = 0$. Let $C(x, t)$ be the inter-

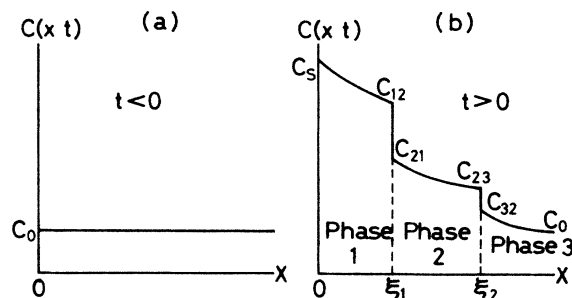


FIG. 3. A model of the staging transition by diffusion in a three-phase system with two moving boundaries. (a) Concentration of intercalants before the onset of intercalation reaction. (b) Concentration of intercalants after the onset of the phase separation into three phases due to the intercalation reaction (phases 1, 2, and 3 correspond to stage 1, stage 2, and higher stages, respectively).

calant concentration in the specimen at position x at time t after the sudden increase in the electrochemical potential from zero to μ . The system is separated into three phases; phase 1 is the stage-1 region, phase 2 the stage-2 region, and the phase 3 is the stage-3 and higher-stage region, respectively. We now have the three diffusion equations for the respective phases:

$$\frac{\partial C}{\partial t} = D_i \frac{\partial^2 C}{\partial x^2} \quad (1)$$

($i=1$ for $0 < x < \xi_1$, $i=2$ for $\xi_1 < x < \xi_2$, and $i=3$ for $\xi_2 < x$), where D_1 , D_2 , and D_3 are the diffusion constants within phase 1 (stage 1), phase 2 (stage 2), and phase 3 (stage 3 and higher stages), and ξ_1 (ξ_2) is the location of the phase boundary between stage 1 (stage 2) and stage 2 (stage 3 and higher stages) regions, respectively. D_i may be approximated as density independent, since the intercalant density changes by 30% at most in a given phase of the present system. Since the sample consists of single phase initially, the initial condition is

$$C = C_0 \text{ for } x > 0 \text{ and } t = 0, \quad (2)$$

and the boundary conditions are

$$C = C_s \text{ for } x = 0 \text{ and } t > 0, \quad (3)$$

$$C = C_{12} \text{ for } x = \xi_1 - 0, \quad (4)$$

$$C = C_{21} \text{ for } x = \xi_1 + 0, \quad (5)$$

$$C = C_{23} \text{ for } x = \xi_2 - 0, \quad (6)$$

$$C = C_{32} \text{ for } x = \xi_2 + 0. \quad (7)$$

The diffusing substance is conserved at the phase boundary so that

$$(C_{12} - C_{21})d\xi_1 = \left[-D_1 \left(\frac{\partial C}{\partial x} \right)_{\xi_1-0} + D_2 \left(\frac{\partial C}{\partial x} \right)_{\xi_1+0} \right] dt, \quad (8)$$

at $x = \xi_1$, and

$$(C_{23} - C_{32})d\xi_2 = \left[-D_2 \left(\frac{\partial C}{\partial x} \right)_{\xi_2-0} + D_3 \left(\frac{\partial C}{\partial x} \right)_{\xi_2+0} \right] dt, \quad (9)$$

at $x = \xi_2$. Above two boundary conditions, Eqs. (8) and (9) can be satisfied for all values of t , if and only if $\xi_i/t^{1/2}$ ($=2\gamma_i D_i^{1/2}$, $i=1,2$) is constant.^{24,25} Particular integrals of diffusion equations (1) contain six parameters besides diffusion constants D_i . Hence, if the concentrations C_0 , C_s , C_{12} , C_{21} , C_{23} , and C_{32} are known, γ_1 and γ_2 can be determined and the three equations (1) can be solved as functions of x and t from the above eight initial and boundary conditions, (2)–(9). The quantities C_{12} , C_{21} , C_{23} , and C_{32} for the H_2SO_4 GIC's have been evaluated as 0.714, 0.410, 0.337, and 0.247, respectively, from Raman scattering study by Eklund *et al.* on the staging kinetics in the H_2SO_4 GIC.^{12,26} Here it is assumed that the concentrations at stage boundaries become the highest or lowest concentration for each stage index. This assumption is based on the fact that a wide range of concentration is realized for a given stage-index region during in-

tercalation. The above concentration at phase boundaries correspond to the chemical formulas of C_{28}X , C_{48}X , C_{60}X , and C_{81}X , respectively [$\text{X} = \text{HSO}_4^- (\text{H}_2\text{SO}_4)_{2.5}$].¹² The concentration is normalized at the composition of C_{20}X which corresponds to the saturated stage 1. Our measurements refer to the staging transition from graphite to stage 1 after the sudden increase in the electrochemical potential. Hence, $C_0 = 0$. The concentration at the interface, C_s , is given as a parameter which is controlled by the electrochemical potential in the present experiment.

The above diffusion problem can be solved numerically, and the results are shown by the solid lines in Figs. 2(a) and 2(b) as a function of DSS. Figure 2(a) shows $\gamma_1 = \xi_1/2\sqrt{D_1 t}$, $\gamma_2 = \xi_2/2\sqrt{D_2 t}$, and Fig. 2(b) shows $(\xi_2 - \xi_1)/\xi_1$. The numerical results agree with experiments within the accuracy of measurements. In the present calculation, the diffusion constant in each of the phases 1, 2, and 3 is set equal to each other so that $D_1 = D_2 = D_3$. The diffusion constant D_1 is obtained as 0.128 mm²/sec by fitting γ_1 to the experimental results.

The density profiles for two cases of DSS or the surface concentration C_s are displayed in Fig. 4 as a function of time. The results for $C_s = 1$ ($C_s = 0.74$) are shown on the left (right) in Fig. 4. The regions of a gradual change in C are seen in each of the phases; stage 1, stage 2, and higher-stage phase from the left to the right in the figure. When DSS is high, for example, $\Delta\mu/\mu_0 = 1.35$ ($C_s = 1$), the specimen contains a wide region of the stage-1 phase.

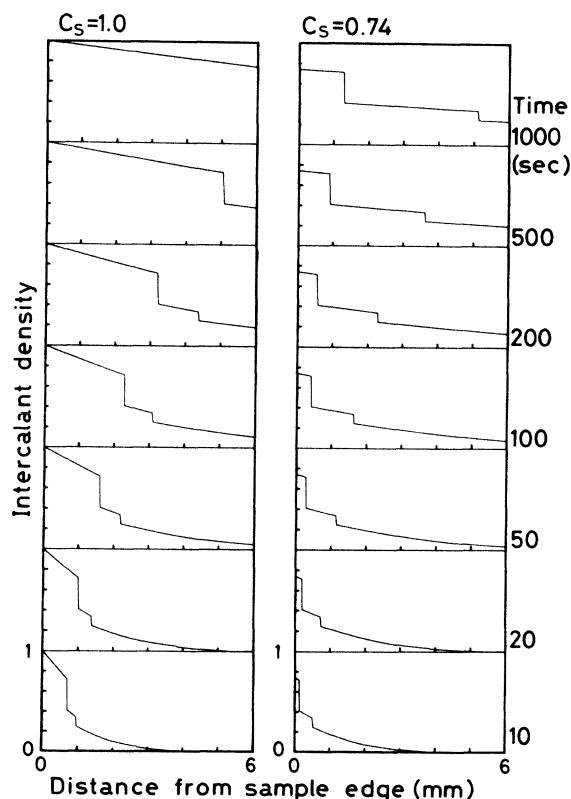


FIG. 4. The time dependence of the concentration profiles for the stages 1, 2, and higher. Left column: $C_s = 1.0$ (DSS equals 1.35). Right column: $C_s = 0.74$ (DSS equals 0.123).

On the other hand, the region of the stage-2 phase increases as DSS decreases, or the chemical potential of the reservoir is close to the phase boundary between stages 1 and 2 in a phase diagram. This dependence on DSS indicates that the distribution of the stage domain is diffusion limited in the phase-1 region which is near the interface. The present results clearly demonstrate that the chemical potential of the reservoir has a great influence on the intercalation process.

In the present simulation we consider the case of a semi-infinite system for simplicity of calculation. The ratio of the length of a given stage region to that of another stage region, i.e., $(\xi_2 - \xi_1)/\xi$, is independent of time in this case. In a finite system of a real experimental arrangement, a higher-stage region disappears at the other end of the sample, and finally all regions of the sample become the stage-1 domain. The present calculation assumes that the concentration at the phase boundary is a

fixed constant throughout the intercalation process. In this case the change in the concentration of each phase limits the staging kinetics as shown in this paper. If the change in the concentration of phase 1 near the reservoir is small without the above restriction at the phase boundary, most parts of the sample may be occupied with the stage-2 region before transition from stage 2 to 1 takes place. At the same time the stage-3 region is transformed into stage 2. The determination of the concentration at the phase boundaries during staging transition would be of considerable interest in the microscopic theory of the staging kinetics.

We gratefully acknowledge Dr. M. Uwaha and Dr. H. Miyazaki for useful discussion, and Dr. A. W. Moore for supplying HOPG crystals. The present work was supported by a Grant-in-Aid for Scientific Research from the Ministry of Education, Science and Culture in Japan.

¹M. S. Dresselhaus and G. Dresselhaus, *Adv. Phys.* **30**, 139 (1981).

²S. A. Solin, *Adv. Chem. Phys.* **49**, 455 (1982).

³R. Clarke and C. Uher, *Adv. Phys.* **33**, 469 (1984).

⁴S. A. Safran, *Phys. Rev. Lett.* **44**, 937 (1980).

⁵S. E. Millman and G. Kirczenow, *Phys. Rev. B* **26**, 2310 (1982).

⁶R. Nishitani, Y. Uno, and H. Suematsu, *Phys. Rev. B* **27**, 6572 (1983).

⁷M. E. Meisenheimer and H. Zabel, *Phys. Rev. B* **27**, 1443 (1983).

⁸R. Nishitani, Y. Uno, and H. Suematsu, *Synth. Met.* **7**, 13 (1983).

⁹W. Metz, P. Josuks, and U. Kleimann, *Synth. Met.* **7**, 319 (1983).

¹⁰M. E. Misenheimer and H. Zabel, *Phys. Rev. Lett.* **54**, 2521 (1985).

¹¹R. Nishitani, K. Suda, and H. Suematsu, *J. Phys. Soc. Jpn.* **55**, 1601 (1986).

¹²P. C. Eklund, C. H. Olk, F. J. Holler, J. G. Spolar, and E. T. Arakawa, *J. Mater. Res.* **1**, 361 (1986).

¹³R. Nishitani, Y. Sasaki, and Y. Nishina, *J. Phys. Soc. Jpn.* **56**,

1051 (1987).

¹⁴H. J. Kim and J. E. Fisher, *Phys. Rev. B* **33**, 4349 (1986).

¹⁵H. J. Kim, J. E. Fischer, D. B. McWhan, and J. D. Axe, *Phys. Rev. B* **33**, 1329 (1986).

¹⁶G. Forgacs and G. Uimin, *Phys. Rev. Lett.* **52**, 633 (1984).

¹⁷P. Hawrylak and K. R. Subbaswamy, *Phys. Rev. Lett.* **53**, 2098 (1984).

¹⁸G. Kirczenow, *Phys. Rev. Lett.* **52**, 437 (1984).

¹⁹G. Kirczenow, *Phys. Rev. Lett.* **55**, 2810 (1985).

²⁰H. Miyazaki, T. Watanabe, and C. Horie, *Phys. Rev. B* **34**, 5736 (1986).

²¹S. Miyazima, *Synth. Met.* **12**, 155 (1985).

²²N. D. Daumas and A. Herold, *C. R. Acad. Sci. C* **268**, 373 (1969).

²³M. S. Dresselhaus and G. Dresselhaus, in *Light Scattering in Solids III*, edited by M. Cardona and G. Guntherodt (Springer, Berlin, 1982), Chap. 2, p. 3.

²⁴R. Nishitani, Y. Sasaki, and Y. Nishina (unpublished).

²⁵W. Jost, *Diffusion in Solids, Liquids, Gases* (Academic, New York, 1960), Chap. I.

²⁶J. O. Bessenhard, E. Wudy, H. Moewald, J. J. Nickl, W. Biberacher, and W. Foag, *Synth. Met.* **7**, 185 (1983).